

Relationship between planar GaAs nanowire growth direction and substrate orientation

This article has been downloaded from IOPscience. Please scroll down to see the full text article.

2013 Nanotechnology 24 035304

(<http://iopscience.iop.org/0957-4484/24/3/035304>)

View [the table of contents for this issue](#), or go to the [journal homepage](#) for more

Download details:

IP Address: 130.126.32.13

The article was downloaded on 04/01/2013 at 03:37

Please note that [terms and conditions apply](#).

Relationship between planar GaAs nanowire growth direction and substrate orientation

Ryan S Dowdy¹, Donald A Walko² and Xiuling Li¹

¹ Department of Electrical and Computer Engineering, Micro and Nanotechnology Laboratory, University of Illinois, Urbana, IL 61801, USA

² Advanced Photon Source, Argonne National Laboratory, Argonne, IL 60439, USA

E-mail: xiuling@illinois.edu

Received 2 August 2012, in final form 13 November 2012

Published 21 December 2012

Online at stacks.iop.org/Nano/24/035304

Abstract

Planar GaAs nanowires are epitaxially grown on GaAs substrates of various orientations, via the Au-catalyzed vapor–liquid–solid mechanism using metal organic chemical vapor deposition. The nanowire geometry and growth direction are examined using scanning electron microscopy and x-ray microdiffraction. A hypothesis relating the planar nanowire growth direction to the surface projections of $\langle 111 \rangle$ B crystal directions is proposed. GaAs planar nanowire growth on vicinal substrates is performed to test this hypothesis. Good agreement between the experimental results and the projection model is found.

[S] Online supplementary data available from stacks.iop.org/Nano/24/035304/mmedia

(Some figures may appear in colour only in the online journal)

1. Introduction

Nanowires have garnered much interest for their potential use in next-generation electronic and optical devices. They have exhibited excellent material quality [1], ease of fabrication [2], and well-defined geometries [3]. Vapor–liquid–solid (VLS) growth, a popular semiconductor nanowire formation method [4], utilizes a metallic nanoparticle catalyst to facilitate nanowire growth. The VLS growth method allows the synthesis of one-dimensional nanostructures with diameters corresponding to the metallic nanoparticle's size. One of the major drawbacks of typical VLS nanowire growth is its incompatibility with traditional planar processing [4]. This is because VLS nanowires are usually grown normal to the surface and require non-trivial [5–7] and potentially costly processes to manipulate the nanowires into a compatible planar format. In addition, nanowires lose their registry to each other when relying upon external alignment processes after their removal from the native substrates.

Previously, our research group has demonstrated the ability to grow planar GaAs nanowires on (100) GaAs substrates [8]. Planar nanowires are epitaxially attached

to their substrates along the length of their axes. This epitaxial connection forces the nanowires to grow in specific crystal directions with full registry to the substrate. Their in-plane arrangement provides a potential solution to some of the compatibility problem. Electrical devices such as MESFETS [9, 10] and HEMTs [11] have been fabricated using planar nanowires on GaAs(100) substrates, demonstrating excellent material quality and good device performance. The downside to planar nanowire technology on (100) substrates is the nanowire growth direction is bi-directional; each individual nanowire has equal probability of growing in one of two anti-parallel $\langle 110 \rangle$ directions. This makes site-controlled growth of planar nanowire arrays on (100) difficult, as the theoretical best yield of a particular nanowire direction is 50%. Recently, we have reported unidirectional growth and electrical performance of planar GaAs nanowires on GaAs(110) substrates [10], thus eliminating the issue of bi-directionality and finding a solution to achieve site-controlled planar nanowire arrays.

In this paper we examine in detail the effect of substrate orientation on the growth direction of planar GaAs nanowires. We measure and analyze the growth direction and topography

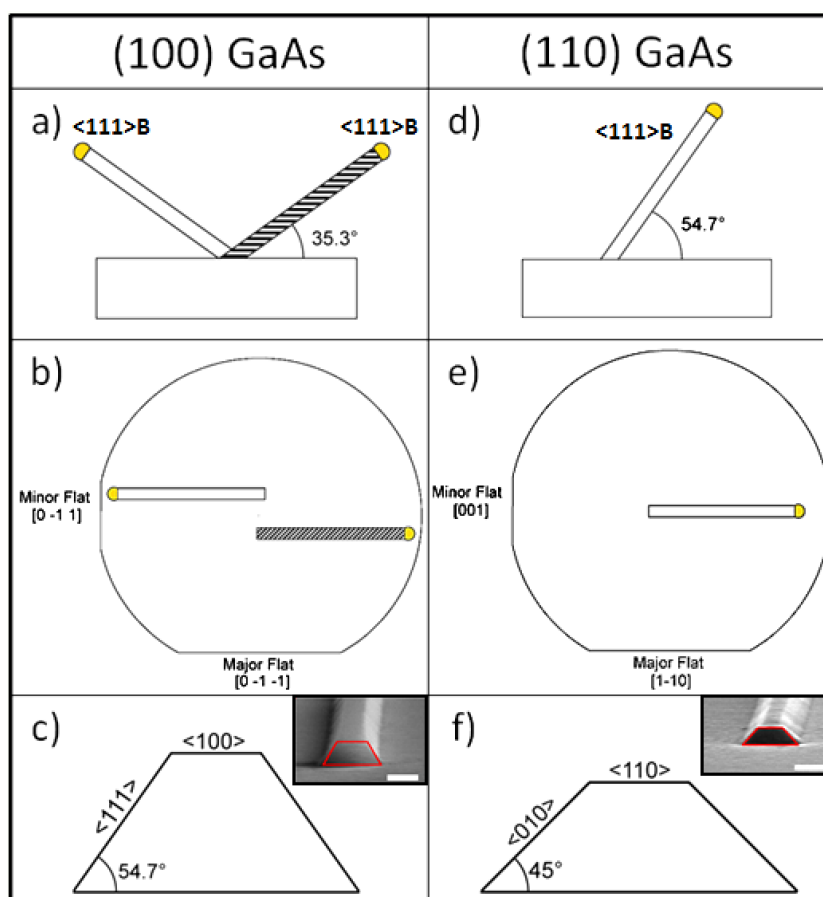


Figure 1. Illustrative comparison of crystal orientations between Au-catalyzed GaAs nanowires grown on GaAs(100) and (110) substrates. ((a), (d)) Available (111) B off-plane nanowire directions with their respective nanowire-to-substrate angles as labeled; ((b), (e)) available growth directions for planar nanowires on their substrates with the wafer flats identified, and ((c), (f)) the cross section geometry of planar nanowires with crystal facets labeled, and SEM images as insets. The scale bar for both insets is 200 nm.

of the nanowires on on-axis (100) and (110), as well as vicinal substrates by x-ray microdiffraction and scanning electron microscopy. We present and verify a theory that uses the in-plane projection of $\langle 111 \rangle B$ to predict the planar nanowire growth direction on semiconductor crystalline substrates.

2. Experimental details

Planar GaAs nanowires were grown on semi-insulating GaAs substrates with three different orientations using a metal-organic chemical vapor epitaxy (MOCVD) reactor. The substrates chosen for this study were on-axis (100), 10° off-cut (100), and (110) substrates. The off-cut angle was defined by the manufacturer (AXT, Inc.) by tilting a GaAs(100) crystal ingot 10° towards the $[0\bar{1}0]$ direction. Preparation for nanowire growth began by dispersing 250 nm colloidal Au nanoparticles on the surface of the substrates. Au nanoparticles were dispersed in an aqueous solution which was evaporated at 115 °C on a hotplate, leaving behind a random distribution of Au nanoparticles on the surface of the substrates. Arsine (AsH_3) was used as the group V precursor and trimethylgallium (TMGa) was used as the group III precursor. The reactor pressure during growth was set at 1013 mbar. Samples were heated to 625 °C under

AsH_3 overpressure to desorb native oxides on the substrate surface and promote alloying between the Au nanoparticles and the GaAs substrates. Samples were then cooled to a temperature of 480 °C to begin nanowire growth. Typical AsH_3 and TMGa flows were 8.93×10^{-4} and 2.49×10^{-5} mol min^{-1} , respectively, with a nominal V/III ratio of 90. After growth, samples were cooled under AsH_3 overpressure. Visual inspection after nanowire growth was performed with a Hitachi S-4800 field emission scanning electron microscope to examine the physical characteristics of nanowires.

X-ray microdiffraction experiments were performed at Beamline 7ID of the Advanced Photon Source at Argonne National Laboratory. Kirkpatrick-Baez mirrors focused the 10 keV x rays to a 30 μm diameter spot at the center of rotation of a six-circle goniometer. However, grazing incidence geometry was used for some measurements to enhance surface sensitivity, which extended the x-ray footprint across the surface of the sample. The resulting x-ray diffraction data reflects an ensemble average of many nanowires. Once a sample was mounted on the goniometer, the orientation of the surface normal was determined by the usual technique of specularly reflecting a laser beam off the surface, and adjusting the chi and phi angles of the Eulerian

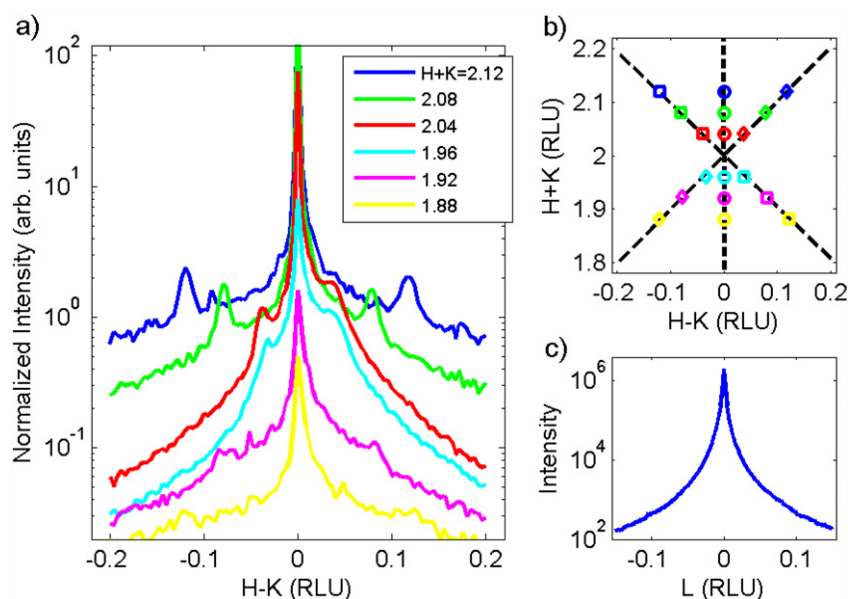


Figure 2. X-ray diffraction scans to determine the orientation of GaAs nanowires grown on a GaAs(110) substrate. The Miller indices are referenced to the substrate crystal lattice. (a) In-plane scans near the (111) Bragg peak, with a large angle of incidence. Scans are in the $[+H, -H, 0]$ direction, i.e., transverse to the nanowires, at various out-of-plane momentum transfer values (indexed as $H + K$ in the legend). Scans are normalized and offset, to be able to display them on the same axes. (b) Map in the $L = 1$ plane of reciprocal space of the peak positions (symbols) and linear best fits (dashed lines). The central peaks (at $H - K = 0$) are from the truncation rod of the flat substrate surface, while the rotated rods ($\pm 45^\circ$) arise from the two angled sides of the trapezoidal nanorods. (c) In-plane scan in the $[00L]$ direction, i.e., along the nanowire growth direction. Scan performed near the $(2, 2, 0)$ Bragg peak at $H = 2.03$ and $K = -1.97$, with an angle of incidence of 0.2° for enhanced surface sensitivity.

cradle until the reflected beam does not move upon rotation about the theta axis [12]. With knowledge of these positions of chi and phi, the direction of the surface normal is then calculated once the crystallographic orientation is determined.

3. Results and discussion

We first analyze the crystal orientations of the most commonly reported out-of-plane and in-plane nanowires grown by the VLS mechanism and summarize in figure 1. On GaAs(100) substrates, out-of-plane VLS nanowire growth favors nanowires propagating in the $\langle 111 \rangle$ B crystal direction (35.3° from the surface) [13], as illustrated in figure 1(a). These GaAs(111) nanowires exhibit bi-directional growth resulting from the two available $\langle 111 \rangle$ B crystal directions available on the surface of (100), specifically, $[11\bar{1}]$ and $[\bar{1}11]$. Planar nanowires on (100) substrates exhibit the same bi-directionality, growing in either the $[01\bar{1}]$ or $[0\bar{1}1]$ crystal directions [13], as illustrated in figure 1(b). The cross-sectional profiles of planar $\langle 110 \rangle$ nanowires on (100) substrates have been identified as trapezoidal with a top $\langle 100 \rangle$ facet and two side $\langle 111 \rangle$ A facets that are 54.7° from the surface [11] (figure 1(c)). Note that the facets are only readily apparent under SEM on nanowires that are approximately larger than 150 nm in diameter; nanowires with a diameter that is less than 150 nm tend to have a more circular cross section with unresolved facets [8].

In contrast, on a (110) substrate there is only one available $\langle 111 \rangle$ B direction (figure 1(b)). Under growth conditions

that favor out-of-plane growth, the nanowires grow along the single $\langle 111 \rangle$ B direction at a 54.7° angle off the surface of the substrate (figure 1(b)). With planar growth conditions, planar nanowires unanimously grow in the $[00\bar{1}]$ direction [10], as illustrated in figure 1(e). The realization of unidirectional planar nanowire growth has significant implications since it is now possible to make completely aligned arrays of epitaxial planar nanowires. The cross-sectional profile of the unidirectional planar nanowires is trapezoidal, consisting of a top $\langle 110 \rangle$ facet and two $\langle 100 \rangle$ facets that are 45° from the surface (figure 1(f)).

To further identify the crystal orientations of these planar nanowires on (110) substrates, we have performed x-ray microdiffraction scans. The measured substrate normal of the (110) is $[0.9988, 1, 0.0048]$, which is 0.1976° from the $[110]$ direction. Since these nanowires grow in complete registry with the substrate, their Bragg peaks overlap those of the substrates; instead, we focus our analysis on rods of diffuse scattering [14] from the well-defined facets of the nanowires. The directions of truncation rods have been used to identify the orientation of vicinal facets [15], nanofacets [16], and edges of isolated nanowires [17]. The series of scans in figure 2(a) are collected at various out-of-plane momentum transfers, next to the GaAs(111) Bragg peak and perpendicular to the growth axis of the nanowires. In figure 2(b) we map the positions of the peaks found in each scan. The central peaks are due to the crystal truncation rod running parallel to the surface normal. This rod, appearing at constant in-plane momentum transfer, is due to scattering from the flat substrate and the top surface

of the nanowires. The side peaks' in-plane positions vary with out-of-plane momentum transfer, and linear fits show they make an angle of $45.0^\circ \pm 0.9^\circ$ to normal, i.e., these peaks reflect scattering from the side facets of the planar nanowires. Within our resolution, the two facet rods intercept at the (111) Bragg peak, indicative of unstrained nanowires. In contrast, scans along the nanowire axis have no additional features; the nanowires have no facets or other features which contribute to scattering in this direction. Shown in figure 2(c) is an in-plane scan in the $[00L]$ direction at $H = 2.03$ and $K = -1.97$, i.e., near the $(2, \bar{2}, 0)$. Similar scans near the GaAs(200) Bragg peaks show the same features. The x-ray microdiffraction results thus confirm the nanowire top and side facets orientations.

VLS growth models have been developed to describe nanowire growth using preferential nucleation [18]. These models describe nanowire growth as a layer by layer process with each layer nucleating preferentially at a position along the edge of a nanowire. These nuclei propagate and form new layers, repeating this process and thus forming the nanowire. For vertical $\langle 111 \rangle$ B wires, nanowires grow perpendicular with respect to the direction of the layer propagation (or the layer stacking occurs in the same direction as nanowire growth). For planar GaAs nanowires, the growth interfaces appear to be $\langle 111 \rangle$ B also [18], but the growth direction and growth interface are no longer perpendicular to each other. We have demonstrated that for both (100) and (110) substrates, the number of available planar growth directions correspond directly to the number of available $\langle 111 \rangle$ B for each given surface $\langle 111 \rangle$ B, and planar nanowires appear to grow along the surface projections of $\langle 111 \rangle$ B crystal directions.

We hypothesize that the planar nanowire growth direction is simply the vector projection of the $\langle 111 \rangle$ B growth directions along the surface of the substrate for growth on all substrates under optimized growth conditions [8]. Taking the vector projection of $\langle 111 \rangle$ B crystal directions on the surface of (100) and (110) substrates does yield their respective planar growth directions: $[0, \bar{1}, 1]$ and $[0, 1, \bar{1}]$ on the (100) substrates and $[0, 0, \bar{1}]$ on the (110) substrates. Assuming this hypothesis is true, for an arbitrary substrate, such as a vicinal substrate off-cut to a specific angle, the planar growth direction can be projected by taking available $\langle 111 \rangle$ B crystal directions on the surface and projecting them onto the substrate (see supplementary data available online at stacks.iop.org/Nano/24/035304/mmedia).

To test this model, nanowires were grown on a (100) substrate that is off-cut by 10° towards $[0, \bar{1}, 0]$. As can be seen from figure 3(a), two propagating directions (red and blue colored) are observed. In contrast to growth on on-axis (100) substrates, the two directions are no longer parallel (or anti-parallel), but rather with an intercepting angle of $\sim 165^\circ$ (or $\sim 15^\circ$) as measured from top-view SEM images.

X-ray microdiffraction was used to determine the orientations of the two sets of nanowires with respect to the substrate. These nanowires, unlike those grown on GaAs(100) or (110), are misoriented with respect to the substrate crystal lattice, so their orientations can be directly determined by finding their Bragg peaks. The orientation of

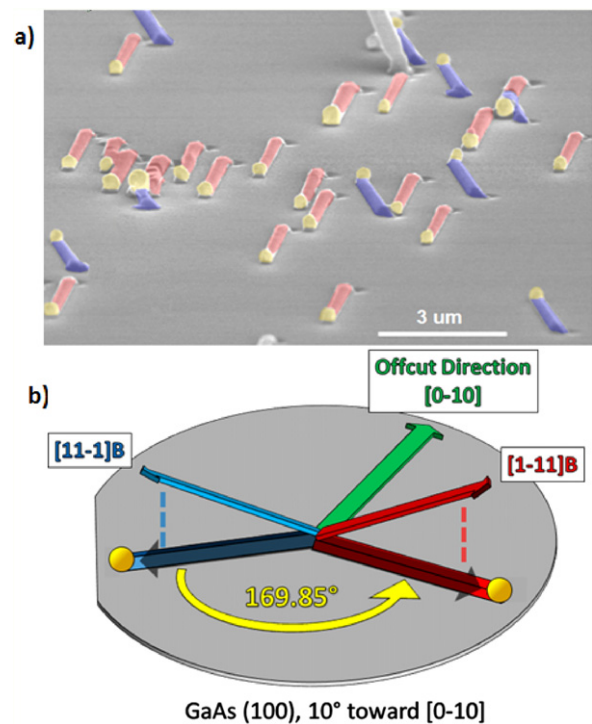


Figure 3. (a) 75° tilted SEM image (false-color) of planar GaAs nanowires grown on a GaAs(100) substrate off-cut by 10° towards $[0\bar{1}0]$, showing two groups of nonparallel planar nanowires. (b) A diagram illustrating the projections of the $\langle 111 \rangle$ B directions onto the substrate, which correspond to the growth directions of the planar nanowires observed in (a). The red-colored planar nanowire is along the projection of $[1\bar{1}]$ B crystal direction and the blue-colored nanowire is along the projection of $[1\bar{1}]$ B crystal direction, as verified by x-ray microdiffraction.

the surface normal was found to be $[0.9846, -0.1747, 0]$, with better than 0.05° accuracy, by comparing the optically specular surface with the crystal orientation of the substrate. Figure 4(a) shows the $[220]$ Bragg peaks of both sets of nanowires, offset by several degrees on opposite sides of the much stronger substrate Bragg peak. In figure 4(b) we place this azimuthal scan in its reciprocal-space context. The growth directions of the nanowires, assumed to be perpendicular to the surface normal, were then found to be $[0.1298, 0.7315, -0.6694]$ and $[-0.0962, -0.5425, 0.8345]$, corresponding to an intercepting angle between the two groups of nanowires of 165.45° as summarized in table 1. The growth directions are also shown in figure 4(b). Also listed in table 1 are values of crystal orientations, $[0.1314, 0.7455, -0.6545]$ and $[-0.1094, -0.6204, 0.7766]$ (thus 169.85° angle between the two nanowire orientations), obtained from the aforementioned vector projection theory and analysis. Good agreement between the calculated projection theory directions and the experimentally derived values are found. Substrate surface morphology such as atomic terraces on off-cut substrates [19, 20], one of the factors the projection model did not consider, could affect the planar nanowire growth direction. However, it is not clear what caused the slight discrepancy between the calculated and measured growth directions at this point. The presence

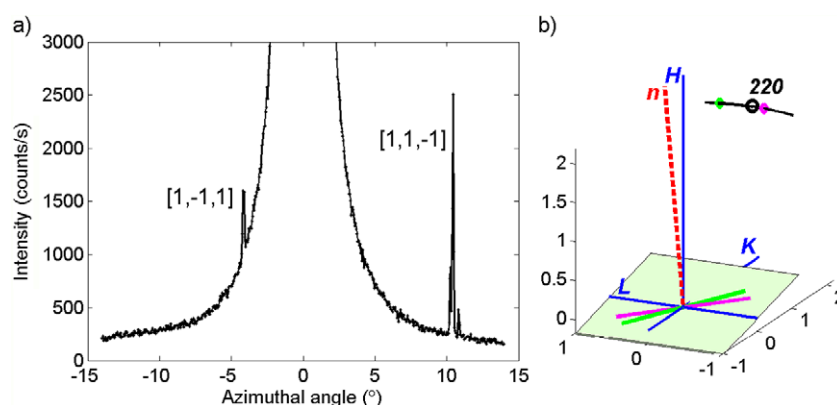


Figure 4. (a) Azimuthal scans around the (220) Bragg peak of a sample with GaAs nanowires grown on a GaAs(100) substrate off-cut by 10° towards $[0\bar{1}0]$. For these scans, the angle of incidence with respect to the surface plane was 2° in order to enhance surface sensitivity. The small peaks on either side of the substrate's central peak are the Bragg peaks of nanowires with growth orientations as labeled. High-resolution scans of these side peaks (not shown) were used to identify the nanowires' exact crystal orientations with respect to the substrate crystal orientation, as described in the text. (b) Reciprocal-space schematic of the azimuthal scan in (a). Major axes of the substrate's reciprocal lattice are shown in blue. The surface normal, n , is shown as a dashed red line, and the light green plane represents the off-cut surface. The 220 Bragg peak is shown as a large circle; the arc cutting through it shows the direction of the azimuthal scan. The locations of the small peaks found in (a) are shown as diamonds; the resulting growth directions of the respective nanowires are shown as lines on the surface plane.

Table 1. A comparison of planar nanowire orientations derived from the vector projection theory mathematically and obtained experimentally from x-ray diffraction for GaAs nanowires grown on a (100) vicinal substrate 10° off-cut towards $[0\bar{1}0]$.

	Calculated direction	X-ray diffraction	SEM visual inspection	Angle difference (deg)
Substrate normal	[0.9848, -0.1736, 0]	[0.9846, -0.1747, 0]	—	0.06
$[1, 1, \bar{1}]$ projected nanowire	[0.1314, 0.7455, -0.6545]	[0.1298, 0.7315, -0.6694]	—	1.17
$[1, \bar{1}, 1]$ projected nanowire	[-0.1094, -0.6204, 0.7766]	[-0.0962, -0.5425, 0.8345]	—	5.62
Angle between planar nanowires	169.85°	165.45°	164.5°	—

of several peaks for the $[1\bar{1}\bar{1}]$ nanowires on the high-angle side of figure 4(a) indicates these nanowires may grow in a small range of orientations, apparently determined by local surface morphology rather than by registry with the substrate lattice. Our results indicate that utilizing vector projection and analyzing available surface growth directions, planar nanowires could theoretically be produced in any orientation, limited only by the substrate orientation itself.

4. Conclusion

In conclusion, GaAs planar nanowire growth direction has been analyzed using three kinds of substrates. Out-of-plane nanowire growth on GaAs substrates occurs in the $\langle 111 \rangle$ B crystal direction while planar nanowires grow along the planar projections of these crystal directions. Limiting the available $\langle 111 \rangle$ B crystal direction is the mechanism that allows unidirectional growth on (110) substrates. X-ray diffraction has been used to unambiguously identify the nanowire crystal direction and cross-sectional geometry as a test of the planar projection theory. Future work will investigate planar nanowire growth for different materials systems and substrate orientations to exemplify the versatility of planar nanowire growth beyond GaAs and fully understand the planar nanowire growth direction on miscut substrates.

Acknowledgments

Financial support was provided in part by NSF DMR award No. 1006581. Use of the Advanced Photon Source, an Office of Science User Facility operated for the US Department of Energy (DOE) Office of Science by Argonne National Laboratory, was supported by the US DOE under Contract No. DE-AC02-06CH11357.

References

- [1] Joyce H J, Gao Q, Tan H H, Jagadish C, Kim Y, Zhang X, Guo Y and Zou J 2007 Twin-free uniform epitaxial GaAs nanowires grown by a two-temperature process *Nano Lett.* **7** 921–6
- [2] Law M, Goldberger J and Yang P 2004 Semiconductor nanowires and nanotubes *Annu. Rev. Mater. Res.* **34** 83–122
- [3] Fortuna S A and Li X 2010 Metal-catalyzed semiconductor nanowires: a review on the control of growth directions *Semicond. Sci. Technol.* **25** 024005
- [4] Goldberger J, Hochbaum A I, Fan R and Yang P D 2006 Silicon vertically integrated nanowire field effect transistors *Nano Lett.* **6** 973–7
- [5] Raychaudhuri S, Dayeh S A, Wang D and Yu E T 2009 Precise semiconductor nanowire placement through dielectrophoresis *Nano Lett.* **9** 2260–6
- [6] Tao A R, Huang J and Yang P 2008 Langmuir–Blodgett of nanocrystals and nanowires *Acc. Chem. Res.* **41** 1662–73

- [7] Pevzner A, Engel Y, Elnathan R, Ducobni T, Ben-Ishai M, Reddy K, Shpaisman N, Tsukernik A, Oksman M and Patolsky F 2010 Knocking down highly-ordered large-scale nanowire arrays *Nano Lett.* **10** 1202–8
- [8] Fortuna S A, Wen J, Chun I S and Li X 2008 Planar GaAs nanowires on GaAs(100) substrates: self-aligned, nearly twin-defect free, and transfer-printable *Nano Lett.* **8** 4421–7
- [9] Fortuna S A and Li X 2009 GaAs MESFET with a high-mobility self-assembled planar nanowire channel *IEEE Electron Device Lett.* **30** 593–5
- [10] Dowdy R, Walko D A, Fortuna S A and Li X 2012 Realization of unidirectional planar GaAs nanowires on GaAs(110) substrates *IEEE Electron Device Lett.* **33** 522–4
- [11] Miao X and Li X 2011 Scalable monolithically grown AlGaAs–GaAs planar nanowire high-electron-mobility transistor *IEEE Electron Device Lett.* **32** 1227–9
- [12] Mochrie S G J 1988 Four-circle angle calculations for surface diffraction *J. Appl. Crystallogr.* **21** 1–4
- [13] Hiruma K 1995 Growth and optical properties of nanometer-scale GaAs and InAs whiskers *J. Appl. Phys.* **77** 447
- [14] Robinson I K and Tweet D J 1992 Surface x-ray diffraction *Rep. Prog. Phys.* **55** 599
- [15] Munkholm A and Brennan S 1999 Influence of miscut on crystal truncation rod scattering *J. Appl. Crystallogr.* **32** 143–53
- [16] Walko D A and Robinson I K 1999 Structure of Cu(115): clean surface and its oxygen-induced facets *Phys. Rev. B* **59** 15446–56
- [17] Diaz A, Mocuta C, Stangl J, Mandl B, David C, Vila-Comamala J, Chamard V, Metzger T H and Bauer G 2009 Coherent diffraction imaging of a single epitaxial InAs nanowire using a focused x-ray beam *Phys. Rev. B* **79** 125324
- [18] Samuelson L, Wacaser B A, Dick K A, Johansson J, Borgstrom M T and Deppert K 2009 Preferential interface nucleation: an expansion of the VLS growth mechanism for nanowires *Adv. Mater.* **21** 153–65
- [19] Leiberich A and Levkoff J 1990 The crystal geometry of $\text{Al}_x\text{Ga}_{1-x}\text{As}$ grown by MOCVD on offcut GaAs(100) substrates *J. Cryst. Growth* **100** 330–42
- [20] Albrechtsen O, Meier H P, Arent D J and Salemink H W M 1993 Terracing and step bunching in interfaces of molecular beam epitaxy-grown (Al)GaAs multilayers *Appl. Phys. Lett.* **62** 2105–7